Journal of Physics: Conference Series

PAPER • **OPEN ACCESS**

CFD simulation of turbulent flows over wire-wrapped nuclear reactor bundles using immersed boundary method

To cite this article: Antonio Cervone *et al* 2020 *J. Phys.: Conf. Ser.* **1599** 012022

View the article online for updates and enhancements.

This content was downloaded from IP address 192.107.67.222 on 29/09/2021 at 18:00

Journal of Physics: Conference Series **1599** (2020) 012022 doi:10.1088/1742-6596/1599/1/012022

CFD simulation of turbulent flows over wire-wrapped nuclear reactor bundles using immersed boundary method

Antonio Cervone[1], Andrea Chierici[2] ,Leonardo Chirco[2], Roberto Da Vià[2†], Valentina Giovacchini[2] and Sandro Manservisi[2]

[1]Italian National Agency for New Technologies, Energy and Sustainable Economic Development, ENEA, Via Martiri di Monte Sole 4, Bologna 40129, Italy
[2]University of Bologna, DIN, Lab. of Montecuccolino, Via dei Colli 16, Bologna 40136, Italy

E-mail: †roberto.davia2@unibo.it

Abstract. A preliminary study for lead-bismuth eutectic (LBE) turbulent flows over wire-wrapped nuclear reactor bundles is performed. The 19-pin hexagonal bundle geometry, representative of NACIE-UP facility and adopted in the MYRRHA reactor [1, 2], is considered. The presence of the helical wire wrap has a strong effect on flow patterns inside the bundle geometry, with induced secondary flows and enhanced mixing [3]. From a computational point of view, the wire-wrapped geometry model is much more complex to realize than the bare rod configuration and simplified models are often used [4, 5]. In order to overcome the difficulties of the model generation, an hybrid body fitted immersed boundary method is used. A computational grid that fits the presence of bundle pins is generated, as for the case of the bare rod configuration, allowing a better control of mesh resolution in the regions close to wall boundaries. The immersed boundary method is used to model the presence of the helical wire wrap so that its effect on fluid motion can be taken into account.

1. Introduction

In the present paper a Lead Bismuth Eutectic turbulent flow occurring inside a wire wrapped 19 pin nuclear reactor bundle is simulated using an immersed boundary approach. This geometry is representative of the NACIE-UP facility and adopted in the MYRRHA reactor, a multipurpose fast neutron spectrum irradiation facility, used as a pilot plant for Lead Cooled Fast Reactors [1, 2]. The presence of the helical wire wrap around the fuel rods has a strong effect on flow patterns inside the bundle geometry, with induced secondary flows and enhanced mixing [3]. For this type of geometry, intended in a more general way as a wire wrapped bundle configuration with an arbitrary number of fuel rods, many investigations have been performed from both experimental and computational points of view. An evaluation of existing experimental correlations for the calculation of pressure drops across wire-wrapped hexagonal array bundles is performed in [6]. Computational Fluid Dynamic (CFD) simulations of turbulent flows inside wire wrapped hexagonal bundles, for several number of pins (from 7 up to 217), have been performed for the cases of liquid sodium and LBE [7, 8, 9, 10, 3, 11]. In these numerical studies the presence of the wrapping wire is investigated in the different effects that it induces: pressure losses, secondary flows that arise in the bundle sub-channels and temperature distributions and related heat transfer coefficients. One major difficulty in simulating these

Content from this work may be used under the terms of the Creative Commons Attribution 3.0 licence. Any further distribution of this work must maintain attribution to the author(s) and the title of the work, journal citation and DOI.
Published under licence by IOP Publishing Ltd

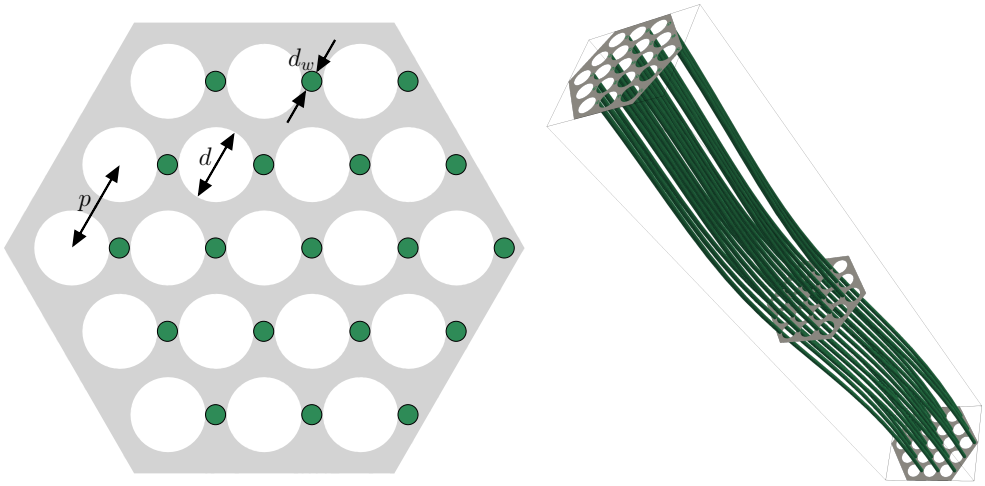

Figure 1. On the left a bundle transversal cross section with highlighted presence of the wrapping wires. On the right the wrapping wires geometry on one helical pitch.

geometries is represented by the generation of a mesh that fits the hexcan wall, the rods and the wrapping wires surfaces [11, 9, 7]. In order to overcome these difficulties, simplifications can be made in terms of the wrapping wires cross section [3, 8, 4, 5].

This paper presents a novel approach to this problem by using an immersed boundary method to model the presence of the wrapping wires, while the equations for mass balance, momentum balance and turbulence model are solved on a computational grid that fits the presence of hexagonal surfaces and the rods. With this strategy the computational grid is more easily generated, with a better control of mesh quality in the near wall region. The purpose of this preliminary study is to investigate the capability of this immersed boundary method to reproduce the key features of the wrapping wires presence, i.e. the enhanced mixing occurring within the sub-channels.

The paper is structured as follows. In Section 2 the immersed boundary method is briefly recalled and extended to the three-dimensional case of a turbulent flow problem. In Section 3 the investigated case is described, together with some of the obtained results. Finally in Section 4 the conclusions that can be drawn from this numerical study are reported.

2. Numerical Modeling

In the present paper a Lead Bismuth Eutectic (LBE) turbulent flow inside a wire wrapped 19 pin nuclear reactor bundle is simulated. In order to study the turbulent behavior the Reynolds Averaged Navier-Stokes (RANS) system of equations is solved and a logarithmic two equation turbulence model is used in order to close the system of equations, obtaining the following

$$\boldsymbol{\nabla} \cdot \mathbf{u} = 0\,, \tag{1}$$

$$\frac{\partial \mathbf{u}}{\partial t} + (\mathbf{u} \cdot \boldsymbol{\nabla})\mathbf{u} = -\frac{1}{\rho}\boldsymbol{\nabla} P + \boldsymbol{\nabla} \cdot \left[(\nu + \nu_t)\left(\boldsymbol{\nabla}\mathbf{u} + \boldsymbol{\nabla}\mathbf{u}^T\right)\right]\,, \tag{2}$$

$$\frac{\partial \mathrm{K}}{\partial t} + \mathbf{u} \cdot \boldsymbol{\nabla}\mathrm{K} = \boldsymbol{\nabla} \cdot \left[\nu^{\mathrm{K}}_{eff}\boldsymbol{\nabla}\mathrm{K}\right] + \nu^{\mathrm{K}}_{eff}\boldsymbol{\nabla}\mathrm{K} \cdot \boldsymbol{\nabla}\mathrm{K} + \frac{P_k}{e^{\mathrm{K}}} + -C_\mu\, e^{\Omega}\,, \tag{3}$$

$$\frac{\partial \Omega}{\partial t} + \mathbf{u} \cdot \boldsymbol{\nabla} \Omega = \boldsymbol{\nabla} \cdot \left[\nu_{eff}^{\Omega} \boldsymbol{\nabla} \Omega \right] + 2\nu_{eff}^{\Omega} \boldsymbol{\nabla} \mathrm{K} \cdot \boldsymbol{\nabla} \Omega + \\ + \nu_{eff}^{\Omega} \boldsymbol{\nabla} \Omega \cdot \boldsymbol{\nabla} \Omega + \frac{c_{\varepsilon 1} - 1}{e^{\mathrm{K}}} P_k - C_{\mu} \left(c_{\varepsilon 2} f_{exp} - 1 \right) e^{\Omega} \tag{4}$$

with $\nu_t = f(\mathrm{K}, \Omega)$. In the system of equations (3-4) the variables K and Ω stand for the logarithmic value of turbulent kinetic energy (TKE) k and the logarithmic value of TKE specific dissipation rate ω. For more details about the turbulence model the interested reader can refer to [12, 13, 14] and references therein. The RANS system of equations (1-2) has been solved using the consistent splitting method presented in [15].

2.1. Immersed Boundary method and turbulence modeling

The generation of a CAD model of both bare bundle configuration and wrapping wires, is represented in Fig. 1. In this paper, the system of equations (1-4) is solved on a computational grid that fits the bare bundle configuration, while the presence of the wrapping wires is modeled using an immersed boundary method. The IB method used in this work has been tested in the past with simulations of laminar flows around static and moving bodies [16] and is here briefly recalled and extended to the three-dimensional case. Let us consider with Ω_s and Ω_f the physical domains occupied by the solid and by the fluid, respectively, so that $\Omega = \Omega_s \cup \Omega_f$ is the whole domain being considered. An indicator function $\chi(\mathbf{x}, t)$ is defined as a multidimensional Heaviside function

$$\chi(\mathbf{x}, t) = \int_{\Omega_s(t)} \delta(\mathbf{x}' - \mathbf{x}) \, d\mathbf{x}' \quad \forall \mathbf{x} \in \Omega \,, \tag{5}$$

where δ is the Dirac delta function. The possible values of $\chi(\mathbf{x}, t)$ over Ω are then

$$\chi(\mathbf{x}, t) = \begin{cases} 1 \,, & \forall \mathbf{x} \in \Omega_s(t) \,, \\ 0 \,, & \forall \mathbf{x} \in \Omega_f(t) \,, \end{cases} \tag{6}$$

so the χ function is used to classify a position $\mathbf{x}$ of the space as occupied by the solid body, when $\chi(\mathbf{x}) = 1$, or occupied by the fluid otherwise. If with Ω^h and Ω_s^h we respectively refer to the computational grids obtained as discretization of Ω and Ω_s, then a discretized indicator function $\chi^h(\mathbf{x})$ can be calculated from the projection of a unitary field from Ω_s^h to Ω^h. The volume fraction field α is a cell-wise field whose values represent the fraction of volume occupied by the solid body for each cell of Ω^h. By using the values of α, the mesh cells of Ω^h can be labeled as fluid, solid or interface cells. A point-wise differentiable field α' is calculated as a Galerkin projection of volume fraction field α, namely

$$\int_{\Omega} \left(\alpha' \phi + \gamma \nabla \alpha' \cdot \nabla \phi \right) d\Omega = \int_{\Omega} \alpha \phi d\Omega \quad \forall \phi \in H^1(\Omega) \,, \tag{7}$$

where γ is an arbitrary diffusion coefficient. The fluid-solid interface is approximated with a plane in those cells where $\alpha \in [0 + \epsilon, 1 - \epsilon]$, where ϵ is an arbitrary threshold value. The unitary vector $\hat{\mathbf{n}}$ normal to the plane approximation of the solid-fluid interface is calculated as the mean integral value of α' gradient inside each interface cell, which means

$$\hat{\mathbf{n}}_i = \int_{\Omega_i} \boldsymbol{\nabla} \alpha' d\mathbf{x} \, / \left| \int_{\Omega_i} \boldsymbol{\nabla} \alpha' d\mathbf{x} \right| , \quad \forall i : \alpha_i \in [0 + \epsilon, 1 - \epsilon] \,. \tag{8}$$

For a given interface cell having $\tilde{n}$ nodes lying in the solid region, namely

$$\chi^h(\mathbf{x}_i) = 1 \,, \quad \forall i = 1, \ldots, \tilde{n} \,, \tag{9}$$

the approximated interface is considered to lay on p-th node, where the p-th node is chosen as the one for which the following rule holds

$$\hat{\mathbf{n}} \cdot (\hat{\mathbf{x}}_p - \hat{\mathbf{x}}_i) < 0 \quad \forall i = 1, \ldots, \tilde{n},\, i \neq p\,. \tag{10}$$

Turbulent quantities, in cells crossed by the solid-fluid interface, are modeled using a cell-representative value of non dimensional wall distance $\tilde{y}^+ = \tilde{y} u_\tau / \nu$, where u_τ is the friction velocity and $\tilde{y}$ is the mean distance between fluid nodes and the plane approximation of solid-fluid interface. The algorithm works as follows. We label with Ω_j^h an interface cell belonging to the computational grid Ω^h. A mean integral velocity vector u_{av} is computed and used to estimate the averaged velocity u_{av}^t along a tangent direction, with respect to the approximated solid-fluid interface, as

$$\mathbf{u}_{\mathbf{av}}^{\mathbf{t}} = \mathbf{u}_{\mathbf{av}} - (\mathbf{u}_{\mathbf{av}} \cdot \hat{\mathbf{n}})\hat{\mathbf{n}}\,. \tag{11}$$

The friction velocity value u_τ is then calculated using the mean tangential velocity modulus $|\mathbf{u}_{\mathbf{av}}^{\mathbf{t}}|$, the computed value of the mean wall distance $\tilde{y}$ and an iterative algorithm based on the typical linear, logarithmic and Musker's velocity profiles [17]. The eddy kinematic viscosity ν_t inside the interface cells is computed using the Musker law, i.e.

$$\frac{\nu}{\nu_t} = \frac{1}{C{y^+}^3} + \frac{1}{\kappa y^+}\,, \tag{12}$$

where C is a constant value, $C = 0.001093$ and κ is the Von Karman constant, $\kappa = 0.41$. As it regards the turbulent quantities K and Ω, on those nodes where $\chi(\mathbf{c}) = 1$, a modified equation is solved, namely

$$\frac{\mathrm{K}^n - ((1-\beta)\mathrm{K}^{n-1} + \beta \mathrm{K}_{mod})}{\Delta t} = \boldsymbol{\nabla} \cdot \left[\nu_{eff}^{\mathrm{K}} \boldsymbol{\nabla} \mathrm{K}\right] + \nu_{eff}^{\mathrm{K}} \boldsymbol{\nabla} \mathrm{K} \cdot \boldsymbol{\nabla} \mathrm{K}\,, \tag{13}$$

$$\frac{\Omega^n - ((1-\beta)\Omega^{n-1} + \beta \Omega_{mod})}{\Delta t} = \boldsymbol{\nabla} \cdot \left[\nu_{eff}^{\Omega} \boldsymbol{\nabla} \Omega\right] + 2\nu_{eff}^{\Omega} \boldsymbol{\nabla} \mathrm{K} \cdot \boldsymbol{\nabla} \Omega + \nu_{eff}^{\Omega} \boldsymbol{\nabla} \Omega \cdot \boldsymbol{\nabla} \Omega\,. \tag{14}$$

In equations (13-14), n designates the time step that is currently been solved, β is a constant value $\beta \in [0, 1]$ and K_{mod}, Ω_{mod} are the modeled values calculated using the cell y^+ value

$$\Omega = \begin{cases} \ln\left(\frac{u_\tau^2}{\nu} \frac{2}{C_\mu y^{+2}}\right) & \text{if } y^+ < 5 \\ \ln\left(\frac{u_\tau^2}{\nu} \frac{1}{\kappa \sqrt{C_\mu} y^+}\right) & \text{if } y^+ > 5 \end{cases} \tag{15}$$

$$\mathrm{K} = \ln(\Omega\, \nu_t)\,. \tag{16}$$

These equations allow a smooth transition of the K and Ω fields between the fluid and the solid regions, avoiding the formation of spurious peaks that could compromise the stability of the numerical solution. The velocity field is set to zero on those nodes that are overlapped with the solid body since the wrapping wires are fixed.

When using a body fitted grid approach, it is difficult to define a meshing strategy that can guarantee a high quality mesh, for example without highly stretched cells or with cells of the same type. The case of the wire wrapped bundle, such as the one that has been considered in this paper, is particularly challenging due to the very thin gaps between the wire and the adjacent pins. By using an immersed boundary method the mesh generation step is greatly simplified since the final grid does not need to conform all the bodies and so a coarser grid can be used. As a consequence, the immersed boundary method is an approximation of CFD

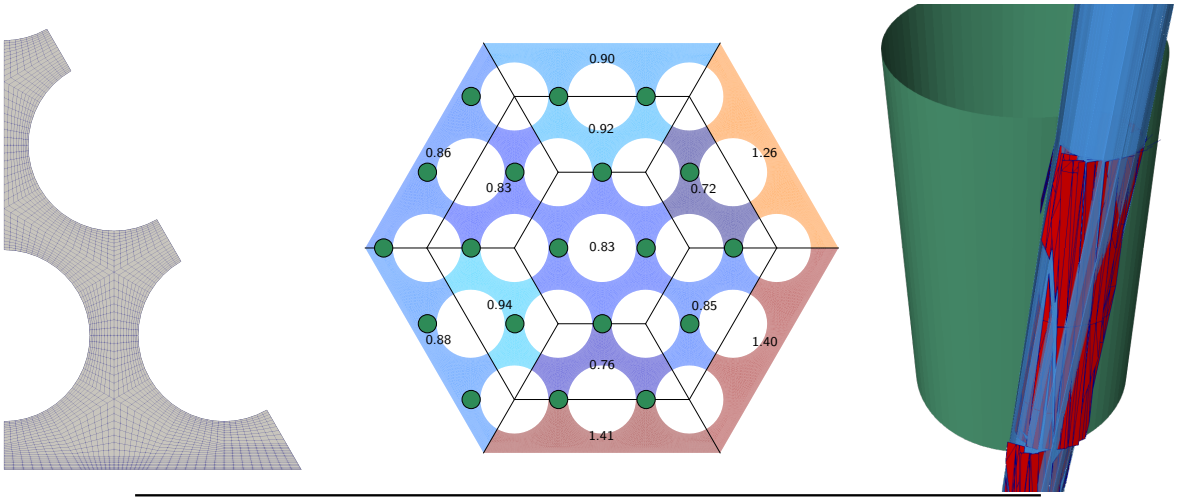

d [mm]	d_w [mm]	$d_{bun,h}$ [mm]	p [mm]	g [mm]	χ [-]	L [mm]
6.55	1.75	4.14	8.4	1.85	1.282	262

Figure 2. Close-up view of the computational grid on a transverse section of the bundle, on the left. On the center the ratio between mean axial velocity component and bulk value for several sub-channels on bundle cross section at z=0.131 m. On the right a reconstructed solid-fluid interface. On the bottom reference values of the geometry characteristic parameters.

studies performed on body fitted mesh, since it requires additional modeling, but allows to do preliminary studies without requiring a huge computational effort.

With respect to a typical CFD approach, some additional fields are required, such as the volume fraction and the color function, together with an interpolation operator between different meshes. For steady cases, the computational effort needed for the implementation of the immersed boundary method is spent just at the beginning of the simulation, since the additional fields do not change during the simulation. The present method has been developed to deal also with moving solid bodies, where volume fraction and color function fields would be updated during the simulation, in order to take into account the body motion. This procedure adds some computational effort, but a body fitted mesh strategy would require additional computational effort too, in the case of mesh moving or re-meshing strategies.

3. Results

In this Section some of the obtained results are presented. The cross section of the simulated geometry is shown on the left of Fig. 1, together with some characteristic parameters, namely the rod diameter d, the distance between adjacent rod center lines p and the wrapping wire diameter d_w. The values of these parameters, alongside the pitch-to-diameter ratio $\chi = p/d$, the helical pitch L, the distance g between the pin outer surface and the hexcan and the bundle hydraulic diameter $d_{bun,h}$ are reported in Table of the Fig. 2. On the right of Fig. 1 the wrapping wires are shown along a complete helical pitch. The fluid mesh used in the simulations consists of 116640 quadratic hexahedral finite elements, with a total of 1000988 nodes, that has been generated as an extrusion, along the z direction, of the bi-dimensional mesh of the bundle cross section, thanks to the exclusion of the wires. Furthermore, with this approach we can refine the mesh along the fuel pin and hexcan walls to better resolve the dynamic boundary layer. The computational grid, on a twelfth of the bundle transverse cross section, is shown in Fig. 2. The length of the geometry, along z direction, is equal to one helical pitch. The immersed boundary

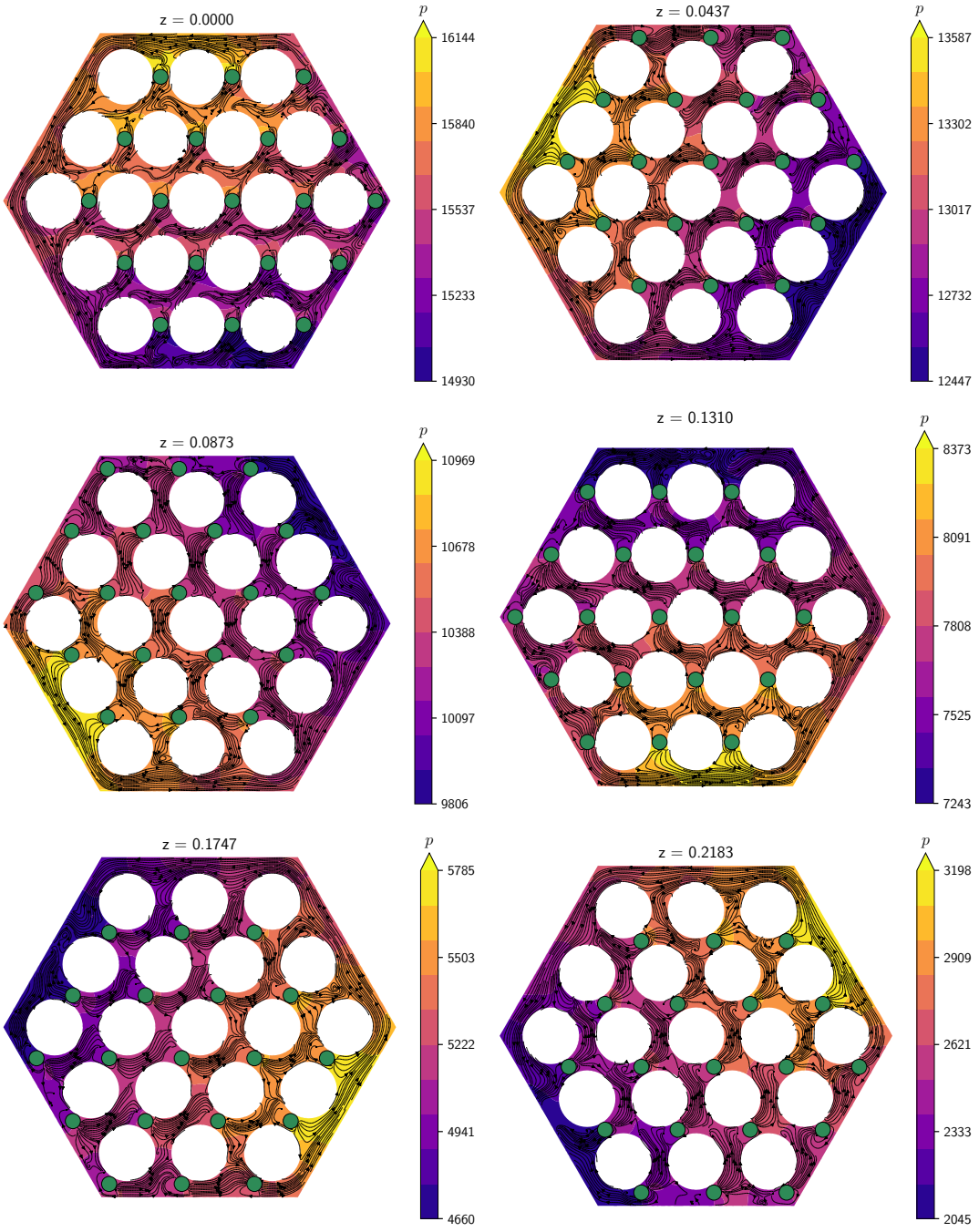

Figure 3. Pressure fields and stream-plots of transverse velocity field at several bundle cross sections along stream-wise coordinates z. The green circles show the position of the wrapping wires.

method, with the newly proposed three dimensional formulation for turbulent flows, has been implemented in FEMuS code [18].

A periodic flow has been solved. Given Γ_{in} and Γ_{out} the inlet and outlet boundaries, respectively, the applied boundary conditions are $\phi\big|_{\Gamma_{in}} = \phi\big|_{\Gamma_{out}}$ and $\boldsymbol{\nabla}\phi\cdot\hat{\mathbf{n}}\big|_{\Gamma_{out}} = -\boldsymbol{\nabla}\phi\cdot\hat{\mathbf{n}}\big|_{\Gamma_{in}}$, where ϕ is a generic solved variable. Since heat transfer is not analyzed, fixed values for density

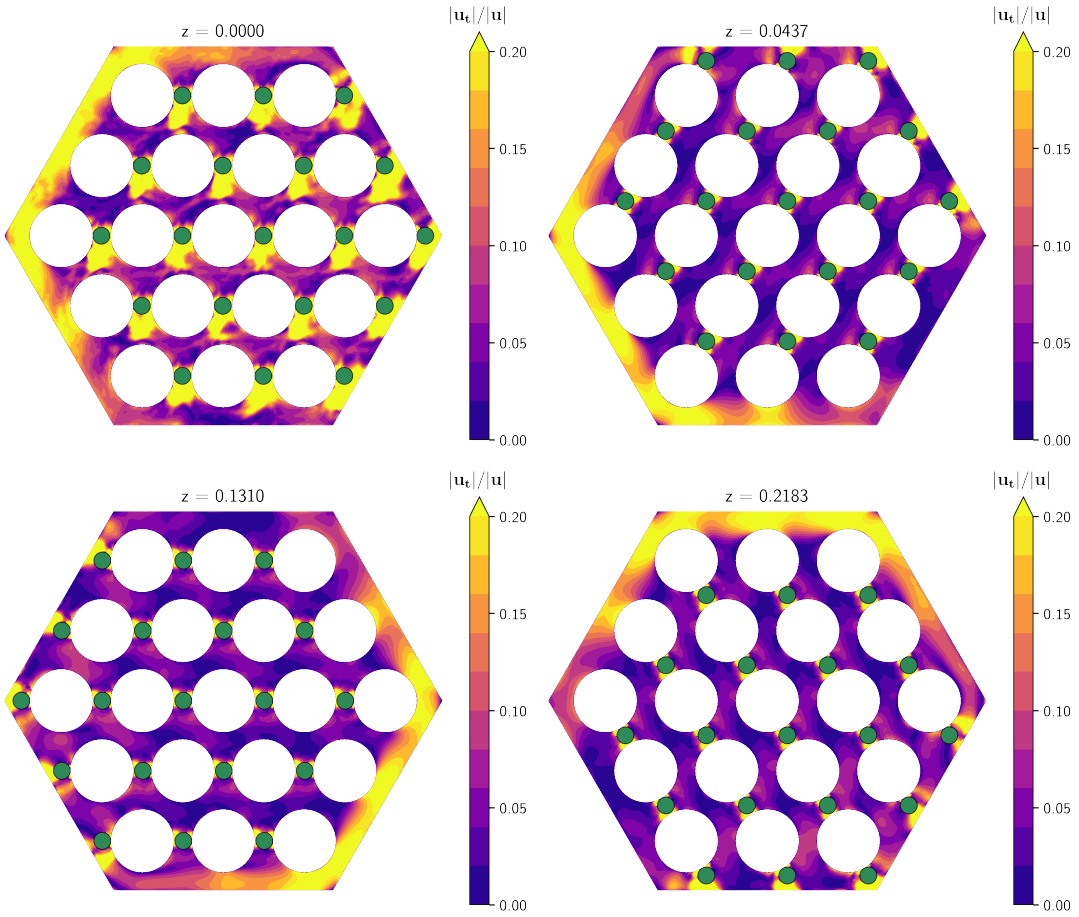

Figure 4. Ratio between transverse and global velocity magnitude on bundle cross sections at several stream-wise coordinates z. The green circles show the position of the wrapping wires.

and dynamic viscosity are used, namely $\rho = 10340 kg/m^3$ and $\mu = 0.001844 Pa\ s$. The mass flow rate is approximately 2.6 kg/s, with a Reynolds number $Re \simeq 9000$, computed using the bundle hydraulic diameter $d_{bun,h}$.

With this study we evaluate the performances of the immersed boundary method in reproducing the key features of the wrapping wire presence. On the center of Fig. 2 the bundle cross section has been divided into several sub-channels, considering a unique central sub-channel and two outer layers, where each outer layer is divided into six different sub-channels. In the Figure the values of the ratio $r = w_{mean}/w_{bulk}$ are shown, where w_{mean} is the average value of the stream-wise velocity component in each sub-channel and w_{bulk} is the bulk stream-wise velocity component value. Finally, on the right of Fig. 2, an example of cell by cell reconstructed solid-fluid interface is shown. The red surfaces represent the planar interface approximating the wrapping wire outer surface, as described in Section 2.1, and a fair representation of the wire boundary is obtained. It can be seen that, as a consequence of the wrapping wire presence, the mass mostly flows through the outer layer sub-channels that are not crossed by the wrapping wires. In Fig. 3 several bundle cross sections taken at different stream-wise locations along z direction are reported, showing the pressure field at each location and the streamlines of the transverse velocity field $\mathbf{u}_t = u\hat{\mathbf{i}} + v\hat{\mathbf{j}}$. As shown, the immersed boundary method is able to reproduce the blocking behavior of the wrapping wires: on each cross-section the pressure shows

a maximum and an opposed minimum that rotate together with the wires. We remark that between adjacent sub-channels the pressure values change when a wire obstructs the flow and the transverse velocity field develops in a counter-clockwise direction in the region close to the hexagonal wall where wrapping wires are not present. In the internal sub-channels vortices arise, enhancing the flow mixing. Fig. 4 shows the distributions of the ratio $|\mathbf{u}_t|/|\mathbf{u}|$ for the same bundle cross sections reported in Fig. 3. An average value of about 0.05 is observed, with peaks occurring in the regions where the wrapping wires almost obstruct the flow section between adjacent sub-channels. These peaks reach values of about 0.2, in agreement with other CFD simulations that can be found in literature [7].

4. Conclusions

In this work we have simulated a Lead Bismuth Eutectic turbulent flow, inside a wire wrapped 19 pin nuclear reactor bundle, with a novel approach that can cope with this complex geometry. A mesh that fits the hexagonal geometry, the fuel rods and the wrapping wires requires a very large number of elements and may suffer of improper resolution due to small gaps and large curvatures. An immersed boundary method has been used to overcome this difficulty and solve the system of governing equations on a mesh generated on the bare bundle configuration. The immersed boundary method is based on a numerical field projection between different meshes that is used to define the mesh cells that are fully occupied by the fluid, fully occupied by the solid or intersected by the solid-fluid interface. The used method is an extension to the three-dimensional and turbulent case of the one previously validated for laminar flows around static and moving objects [16]. Obtained results have shown the ability of the immersed boundary method to capture the key features of the wrapping wire presence, in terms of pressure field distribution, transverse flow streamlines and ratio between transverse and axial velocity fields magnitudes. This model can be considered a starting point for future analyses that will take into account also for the turbulent heat transfer occurring inside the bundle.

References

[1] Tarantino M, Grandis S D, Benamati G and Oriolo F 2008 *J. Nucl. Mater* **376** 409 – 414
[2] Abderrahim H *et al.* 2001 *Nucl. Instrum. Methods Phys. Res* **463** 487 – 494
[3] Gajapathy R, Velusamy K, Selvaraj P, Chellapandi P and Chetal S C 2009 *Nucl. Eng. Des.* **239** 2279–2292
[4] Pacio J, Wetzel T, Doolaard H, Roelofs F and Van Tichelen K 2015 Thermal-Hydraulic Study of LBE-Cooled Fuel Assembly in the MYRRHA Reactor: Experiments and Simulations *International Topical Meeting on Nuclear Reactor Thermal Hydraulics 2015, NURETH 2015* (Chicago) pp 47–60
[5] Pacio J *et al.* 2001 *Nucl. Eng. Des.* **290** 27 – 39
[6] Chen S, Todreas N and Nguyen N 2014 *Nucl. Eng. Des.* **267** 109 – 131
[7] Raj M N and Velusamy K 2016 *Ann. Nucl. Energy* **87** 331 – 349
[8] Fricano J and Baglietto E 2014 *Ann. Nucl. Energy* **64** 32 – 42
[9] Jeong J H, Song M S and Lee K L 2017 *Nucl. Eng. Des.* **313** 470 – 485
[10] Angelucci M, Piazza I and Marinari R 2015 CFD pre-test analysis of the fuel pin bundle simulator experiment in the NACIE-UP HLM facility *International Topical Meeting on Nuclear Reactor Thermal Hydraulics 2015, NURETH 2015* (Chicago) pp 86–100
[11] Chen J *et al.* 2018 *Ann. Nucl. Energy* **113** 256 – 269
[12] Da Vià R, Manservisi S and Menghini F 2016 *Int. J. Heat Mass Tran.* **101** 1030–1041
[13] Da Vià R and Manservisi S 2019 *Int. J. Heat Mass Tran.* **135** 591–603
[14] Manservisi S and Menghini F 2015 *Nucl. Eng. Des.* **295** 251 – 260
[15] Guermond J, Minev P and Shen J 2006 *Comput. Methods Appl. Mech. Eng.* **195** 6011 – 6045 ISSN 0045-7825
[16] Abbati A, Chierici A, Chirco L, Vià R D and Manservisi S 2019 *J. Phys. Conf. Ser.* **1224** 012002
[17] Musker A J 1979 *AIAA Journal* **17** 655–657
[18] Femus code URL `https://github.com/FemusPlatform/femus`